Supplementary Material

S1. Utah Optrode Array Fabrication

The fabrication process flow of the BOROFLOAT33 UOA device is detailed fully in Scharf *et al.*,[1] covered briefly in the main text and supplemented by the figure below.

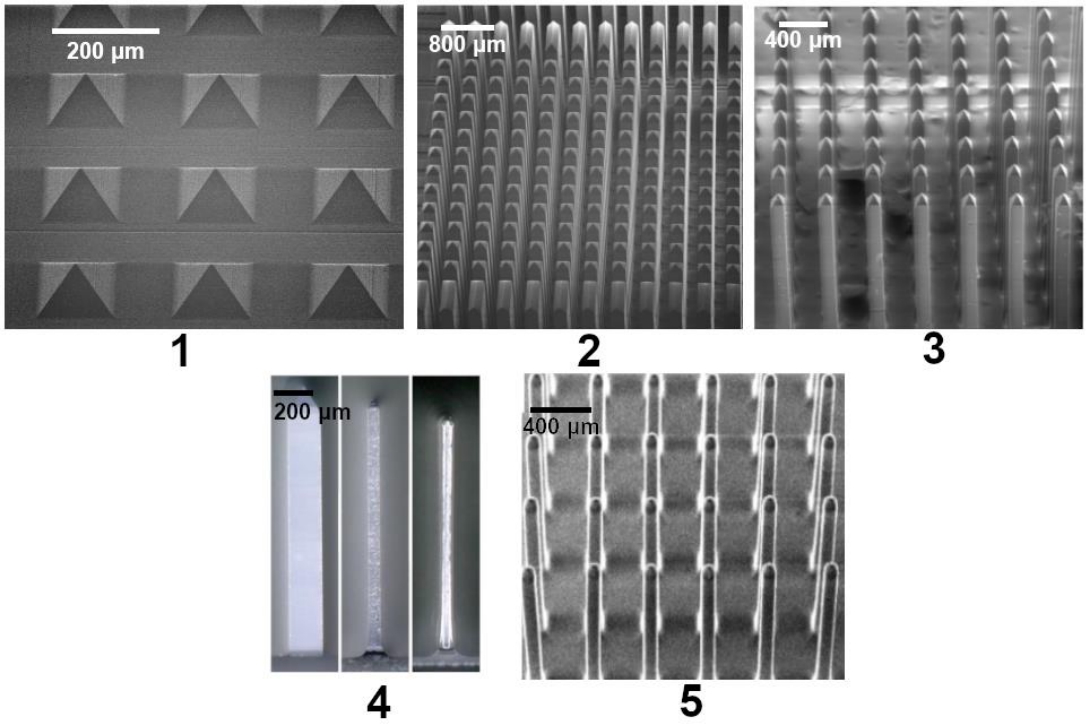

Fig. S1: Step 1 - Tip formation, pyramidal structures are formed using a Disco DAD3220 dicing saw with a bevel blade on 25 mm BOROFLOAT33 glass piece (2.3 mm thickness). Step 2 - Pillar formation, deep kerfs are made in between the pyramid tips to create rectangular pillars. In this case the pillars measure 1.5 mm in height. Step 3 - Chemical etch, 49 % HF: 37% HCl (9:1) solution is used to thin the pillar shanks and smooth the surface. Step 4 – Annealing step, which further smooths the surface and is required to reduce optical scattering along shank length. Left: before chemical etch, middle: after etch (unannealed), right: annealed. Step 5 - SEM of the completed device.

S2. LED Array Fabrication

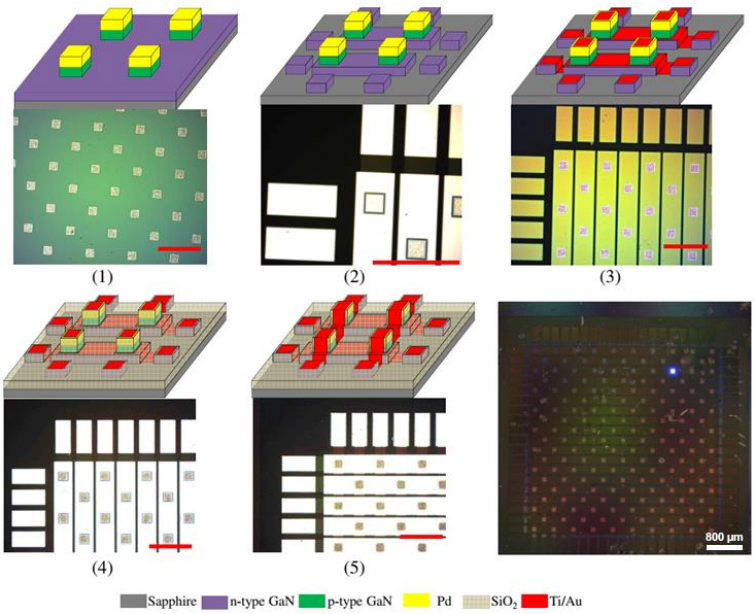

Fig. S2: Fabrication process flow of microLED array (red scale bars are 400 µm). Step 1: A thin Pd layer is deposited using electron-beam evaporation. This layer is then etched using reactive ion etching (RIE) to form the LED p-contact. Following the Pd etch, the p-GaN is etched using an inductively coupled plasma (ICP) system to create the microLED pixels (square with an 80 µm side). Step 2: The n-GaN is now patterned and etched using an ICP etch. Step 3: The sample is annealed using a rapid thermal anneal (450^{o}C). A lift off process is then used to pattern a sputter deposited Ti/Au bilayer. Step 4: A PECVD SiO_2 layer is deposited as an insulation layer between n-tracks and p-tracks. Vias are opened in the SiO_2 with RIE. Step 5: The p-tracks are sputter deposited (Ti/Au) and patterned using a lift off process. A subsequent lift off process patterns the metal bondpads (Ti (100 nm): Pt (200 nm): Au (400 nm)) for wire bonding to control electronics.

S3. Pinhole Patterning and Device Integration

Upon completion of the microLED fabrication, the chip was mechanically thinned from the sapphire side to 150 µm and then diced into individual devices. An individual microLED array was then bonded (Norland NOA 61) to each UOA. As both devices are transparent it is possible to accurately align features on both devices. The effect of misalignment was studied using with optical modelling (Fig. S3C). This indicates that we have a tolerance to misalignment of approximately 10 µm before there is significant loss of optical power coupled into the optrodes. In order to study optical cross talk between adjacent needles, a prototype device with the sapphire-side coated in a metal thin film (Ti:Au, 20nm:30nm) was fabricated. This metal layer had 40 µm square side apertures (patterned using a lift off technique) over the microLED illumination sites – allowing light to pass through and couple into the needles while blocking stray light that would out-couple into tissue. Only half the array was covered with this pinhole layer to allow a direct comparison.

Developing an electrical connection scheme to address each microLED separately is challenging. Therefore, a matrix-addressing scheme was adopted. In this approach, all pixels along one column share a common anode (p-contacts) and all pixels along one row share a common cathode (n-contacts) –Fig. S3A. This means that only 38 connections are required, 19 anodes and 19 cathodes, which simplifies the electronic driver scheme dramatically and allows commercial LED current drivers to be employed. This approach reduces the number of connections, at the cost of limiting the available patterns that can be displayed. For example, individual LEDs, horizontal or vertical lines and rectangles/squares are possible. Diagonal illumination patterns and simultaneously displayed horizontal and vertical lines are not possible. Pulse width modulation schemes can be used to realise these restricted patterns. Each of the 38 connections is linked to LED driver circuitry through a 25 micron insulated gold wire (Fig. S3B). This method of interconnection is widely used in the 100-channel Utah Electrode Array system.[2] The wire-bonds have a length of 10 cm and, since they are insulated, can be bundled together. Silicone (MED 4211, NuSil Technology) can be added to secure the bond connections, increasing the strength of the wire bundle, and further encapsulating the interconnect region. The completed device is shown in Fig. 1 B with the wirebonds encapsulated in this manner.

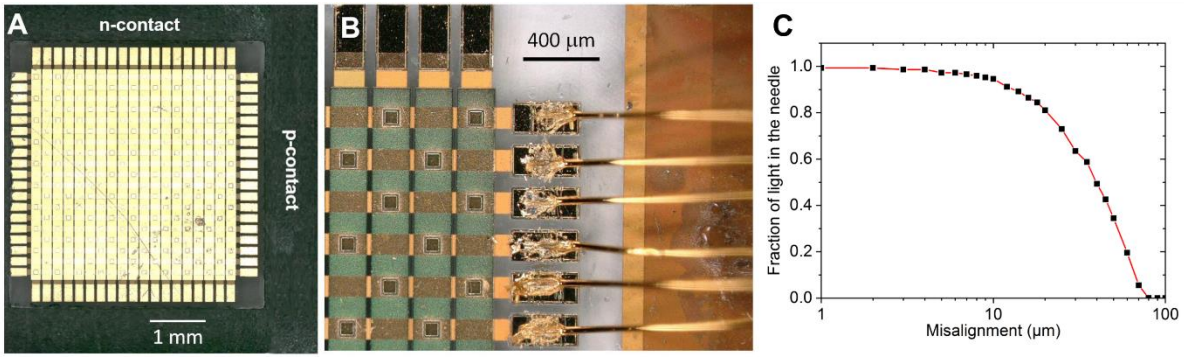

Fig. S3: A) Completed microLED chip showing the 19 n-contacts and 19 p-contacts. The row-column (matrix) addressing scheme reduces the number of interconnects. **B)** Wirebonded device before back surface encapsulation with silicone. **C)** Alignment tolerance of the microLED array to needle array. Power out of the tip of a needle as fraction of the maximum power (0 misalignment).

S4. Interstitial Sites

Addressing the interstitial sites is less of a challenge as we do not have to couple light into an optrode with a limited size and numerical aperture. Fig. S4 details the optical performance of these illumination sites.

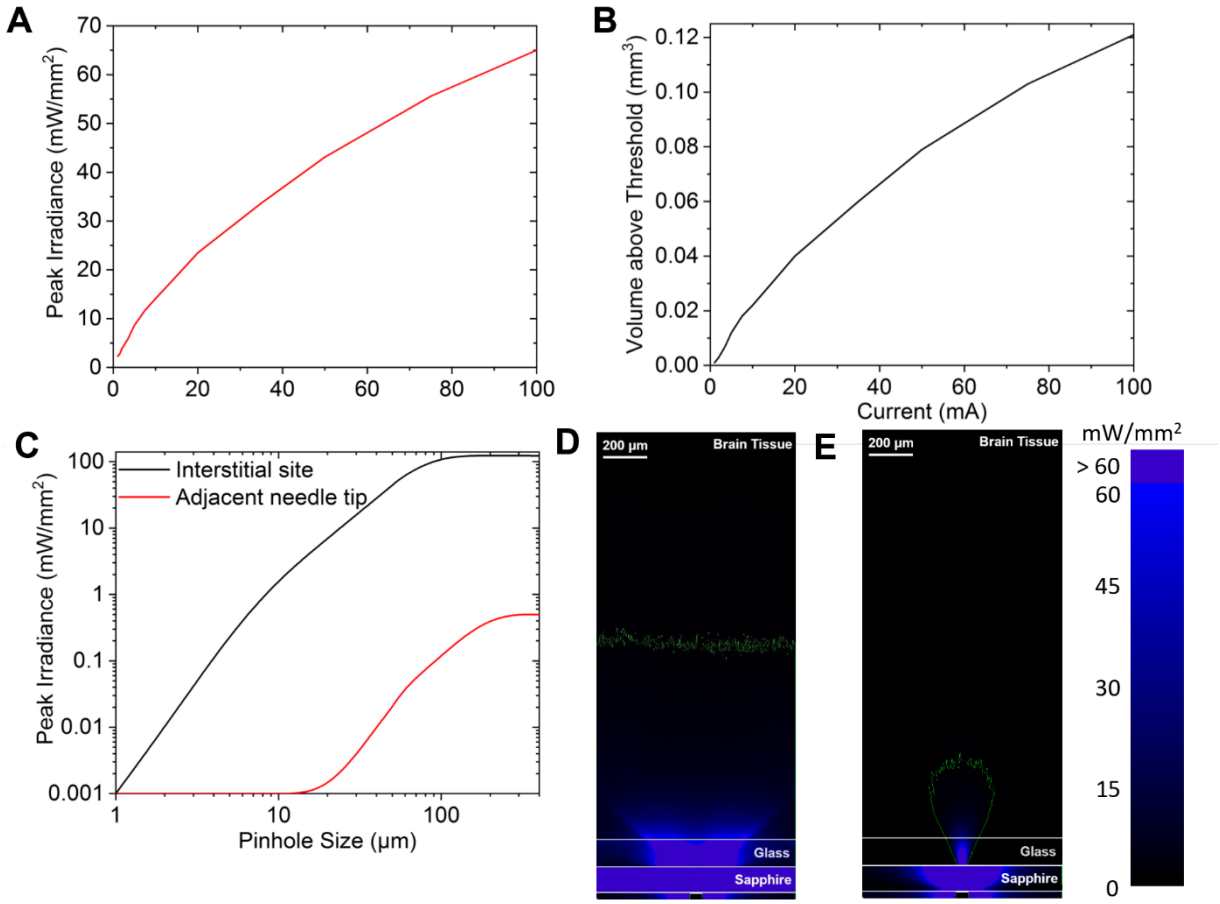

Fig. S4: Measured and Modelled light output from an interstitial site. **A)** Measured peak irradiance for a given microLED current. **B)** Modelled volume above an irradiance threshold of 1 mW/mm^2. **C)** Modelled effect of the pinhole on the light output from an interstitial microLED. For our prototype device a square interstitial pinhole of side 60 µm was chosen. No significant irradiance (>1 mW/mm^2) was detected in needle sites neighbouring the interstitial microLED. **D)** A cross section of the light emission from an interstitial microLED operating at 50 mA with no pinhole layer. **E)** A cross section of the light emission from an interstitial microLED operating at 50 mA with a 60 µm pinhole layer. The green contour line highlights the 1 mW/mm^2 irradiance level taken here as a threshold for ChR2 excitation.

S5. Thermal Limits on Device Performance

Table S1: We detail the thermal restrictions on the reported device across a range of typical operating parameters for optogenetic experiments. A certain microLED current delivers a peak irradiance, illuminating a volume of tissue above 1mW/mm^2. For a given pulse width, the maximum pulse repetition rate is quoted such that the tissue temperature rise is kept below a 1^{o}C increase.

Single LED operated

Device current (mA)	Peak irradiance (mW/mm^2)	Volume above 1mW/mm^2 threshold (mm^3)	Pulse width (ms)	Pulse repetition rate (Hz) with □T<1^{o}C
10 mA	18	0.006	1	1000
			10	100
			100	10
20 mA	30	0.011	1	750
			10	75
			100	7.5
50 mA	56	0.026	1	220
			10	22
			100	2.2
100 mA	80	0.048	1	60
			10	6
			100	0.6

2 LEDs operated simultaneously

Device current (mA)	Peak irradiance (mW/mm^2)	Volume above 1mW/mm^2 threshold (mm^3)	Pulse width (ms)	Pulse repetition rate (Hz) with □T<1^{o}C
10 mA	18	0.012	1	800
			10	80
			100	8
20 mA	30	0.022	1	400
			10	40
			100	4
50 mA	56	0.052	1	110
			10	11
			100	1.1
100 mA	80	0.096	1	30
			10	3
			100	0.3

5 LEDs operated simultaneously

Device current (mA)	Peak irradiance (mW/mm^2)	Volume above 1mW/mm^2 threshold (mm^3)	Pulse width (ms)	Pulse repetition rate (Hz) with □T<1^{o}C
10 mA	18	0.030	1	300
			10	30
			100	3
20 mA	30	0.055	1	150
			10	15
			100	1.5
50 mA	56	0.130	1	40
			10	4
			100	0.4
100 mA	80	0.240	1	10
			10	1
			100	0.1

10 LEDs operated simultaneously

Device current (mA)	Peak irradiance (mW/mm^2)	Volume above $1mW/mm^2$ threshold (mm^3)	Pulse width (ms)	Pulse repetition rate (Hz) with □T<1ºC
10 mA	18	0.060	1	140
			10	14
			100	1.4
20 mA	30	0.110	1	70
			10	7
			100	0.7
50 mA	56	0.260	1	20
			10	2
			100	0.2

20 LEDs operated simultaneously

Device current (mA)	Peak irradiance (mW/mm^2)	Volume above $1mW/mm^2$ threshold (mm^3)	Pulse width (ms)	Pulse repetition rate (Hz) with □T<1ºC
10 mA	18	0.120	1	60
			10	6
			100	0.6
20 mA	30	0.220	1	30
			10	3
			100	0.3
50 mA	56	0.520	1	10
			10	1
			100	0.1

50 LEDs operated simultaneously

Device current (mA)	Peak irradiance (mW/mm^2)	Volume above $1mW/mm^2$ threshold (mm^3)	Pulse width (ms)	Pulse repetition rate (Hz) with □T<1ºC
10 mA	18	0.300	1	20
			10	2
			100	0.2
20 mA	30	0.550	1	10
			10	1
			100	0.1

S6. Alternative Device Configurations

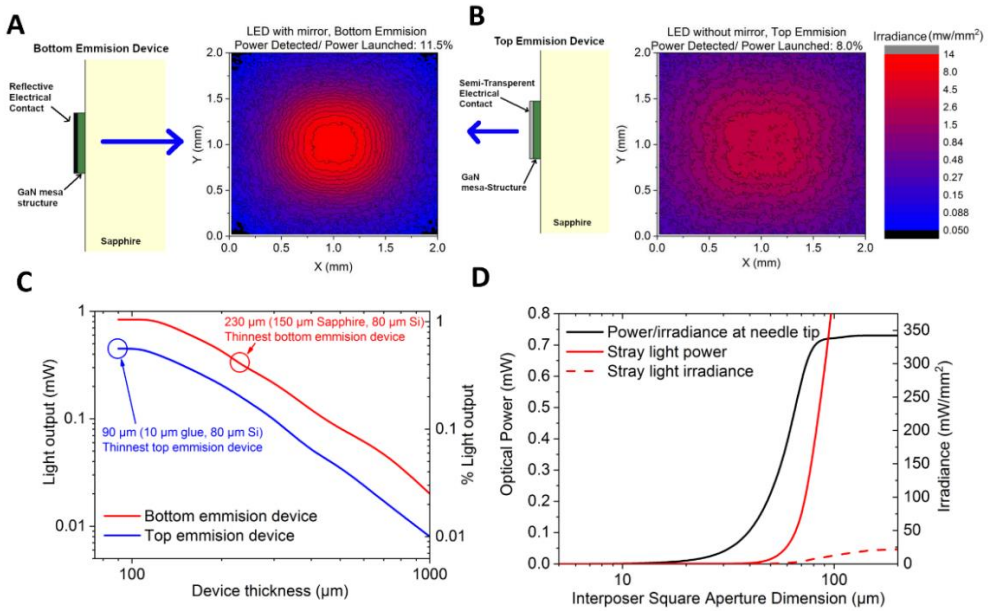

Fig. S5: A) A typical GaN on Sapphire microLED is fabricated so that the electrical contact behaves as a mirror to maximise light output through the sapphire. The modelled beam profile from an 80 µm bottom emission microLED is shown. **B)** It is also possible to produce a top emitting microLED using transparent electrical contacts. The modelled beam profile from an 80 µm top emission microLED is shown. A) and B) share the same irradiance scale. **C)** It is possible to fabricate the UOA on a Si substrate (as opposed to glass) with vias etched to allow light to pass through. We model this optical interposer design and calculate the optical power out of the tip of a needle for both top and bottom emission microLEDs as a function of substrate thickness. Highlighted are the limits of our current fabrication technology. **D)** The power and peak irradiance at the tip of the needle (solid black line) as well as the stray light power (solid red line) and irradiance (dashed red line) are plotted as a function of Si interposer dimension.

Table S2: Summary of the modelled optical efficiencies of the proposed devices. Option 1, is the microLED device reported in the main manuscript coupled to the silicon interposer design. For reference, if 1% of the light was coupled to the needle, it would correspond to a peak irradiance in the tissue of ~ 300 mW/mm^2. In the bottom emission case, 4.2 % of the light is emitted in the opposite direction of the needle. In the top emission cases (options 2-4), this increases to 9.5 %. The difference is due to the electrical contact in the bottom emitting case being thicker and acting as a reflector. In the top emitting case, this contact needs to be kept thin for optical transparency reasons.

Device description	Modelled Light Out of tip (%)	Stray light (%)	Trapped or absorbed light (%)
Option 1: Bottom emission, 150µm sapphire, 80µm silicon, 60µm interposer hole	0.4	0	95.4
Option 2: Top emission, 10µm optical adhesive, 150µm glass, no pinhole	0.3	15.6	74.6
Option 3: Top emission, 10µm optical adhesive, 150µm glass, 40µm pinhole	0.2	1.5	88.8
Option 4: Top emission, 10µm optical adhesive, 80µm silicon, 60µm interposer hole	0.6	0.1	89.8

References (Note: all references are cited in the main text)

1. R. Scharf et al., “A compact integrated device for spatially selective optogenetic neural stimulation based on the Utah Optrode Array.” *SPIE BiOS*. Vol. 10482. 2018: SPIE.

2. X. Xie et al., “Long-term reliability of Al2O3and Parylene C bilayer encapsulated Utah electrode array based neural interfaces for chronic implantation,” *Journal of Neural Engineering* **11**(2), 026016 (2014)